Proceedings of 2009 International Conference on Computational Methods for Energy Engineering and Environment: ICCM3E.
Sousse, Tunisia, 20-22 November, 2009, pp.115-121

The control of natural convection in the horizontal Bridgman configuration under an external magnetic field: symmetric and non-symmetric cross sections

Inès Baaziz[1], Khira Zlaoui[1], Nizar Ben Salah[1] and Daniel Rousse[2].

1 Laboratoire de Mécanique, Matériaux et Procédés, Ecole Supérieure des Sciences et Techniques De Tunis (ESSTT),

5 Avenue Taha Hussein, 1008 Montfleury, Tunis, Tunisie.

2 Chaire de Recherche Industrielle T3E, Ecole de Technologie Supérieure, Université du Québec, Qc, Canada.

***Abstract*—This study deals with electromagnetic braking of free-convective flows in cavities similar to those used in the crystal growth horizontal Bridgman configuration. The cavities are filled with dilute electrically conducting alloy, with a low Prandtl number, and subjected to an horizontal gradient of temperature. The flow is steady and laminar under an external vertical, transversal, and uniform magnetic field.**

A numerical code based on the finite element method has been developed to study the effects of the variation of the Hartmann number Ha on the distributions of the velocity and on the induced magnetic field for a given Grashoff number Gr and for different cross section shapes (symmetric: circle, square, and lozenge and non symmetric: triangle). In the case of non symmetric cross sections, the results show the way the flow is reorganized within the domain.

Results are validated through the comparison with analytical results, in the limit of very high Hartmann numbers, found in literature.

Keywords-component; Free convection; Magnetic field; Magneto-hydrodynamics; Cross section; Solidification; Bridgman configuration.

I. INTRODUCTION

The possibility of mastering the metallurgical structure, as well as the defects which appear during the solidification, allows enhancing materials properties for industrial use. Moreover, multiple use properties (mechanical, chemical, and physical) depend directly on the microstructure. For different steel types, it is always possible to modify the microstructure of solidification by thermo-mechanical treatments during the solid phase later on. However, for semiconductors such an option is out of question and the microstructure of solidification acts directly upon the properties of the resultant material. Thus, the importance of the selection and the control of the microstructure emerge, in order to master the desired properties of the material. The steered solidification processes present a privilege by allowing the check of the crystal growth during the liquid phase, and as a result, the production of mono-crystal alloys of high quality.

Among steered solidification processes, the horizontal Bridgman method (HBM) may be considered for its simplicity compared to the other methods and for its allowance to independently control the three experimental parameters: the temperature gradient, the concentration of the alloy, and the velocity of pulling. In the configuration of horizontal Bridgman, the single crystal develops slowly inside a melting pot of variable geometry, which is subject to an external unidirectional axial thermal gradient and filled with an alloy fluid having an initial concentration C_0. The cavity is pulled with a constant velocity V crossing from its liquid phase in hot zone towards its solid phase in the colder one. A solid-liquid interface takes place permitting, in this way, the distinction between both phases. The gradient of temperature induces free convective movements, acting on the crystalline growth by ordering the transport of doping impurities and of heat in the growth interface. The resulting natural convection, during the crystalline growth, causes non homogeneities and striations which induce defects affecting the quality of the resultant crystals. Thus, the understanding of the movements of natural convection and the ability to control them become an objective to strive for in order to damp them or even to eliminate them. Since the materials in concern are good electrical conductors in their liquid state, using MHD effects becomes a possibility to modify the fluid motion and therefore obtain crystals which better satisfy the ever increasing requirements of technology.

Many studies proved that magnetic fields can be used to damp the convection during the directional solidification of electrically conductive molten materials. The control of the intensity of convection by exposing the convector flow to a magnetic field of constant or variable strength and direction has been put into evidence in many works during the last three decades as in the investigations of Hoshikawa et al. [1] and Kim et al.[2] made for the control of the crystal growth in the Czochralski method. Those works have shown significant improvements of the quality of the crystals of silicon due to the reduction of temperature fluctuation responsible of the oscillating crystal growth characterized by a non uniform distribution of dopant in the crystal.

More recently, the experience of Campbell and Koster [3] on the crystalline growth of pure gallium in the horizontal Bridgman configuration proved that the intensity of the convection may modify the shape of the solidification front. For the same configuration, Davoust et al. [4] investigated numerically the magneto-hydrodynamic MHD control of free convection. The numerical results showed the MHD damping and the reorganization of the convective flow obtained for $0 < Ha < 100$ and illustrated the building-up of the Hartmann layers and the side layers when the Hartmann number increases.

Moreover, the same configuration with a rectangular enclosure was also studied analytically by Garandet et al. [5]. In this 2D analysis, the authors demonstrated that for a high number of Hartmann, the gradient of velocity in the heart of the cavity is always constant, outside both Hartmann layers, and far from walls parallel to the magnetic field.

Later on, in the current decade, many numerical, analytical, and experimental studies have been published. A numerical investigation using p-version least-squares finite element method was developed by Dennis et al. [6] for the prediction of the solidification from a melt under the influence of an externally applied magnetic field. The numerical results showed considerably different flow patterns in the melt and temperature distribution in the resulting solid in both cases of full and reduced gravities.

Mitric et al. [7] studied experimentally the effect of applying an alternating magnetic field on the crystal growth of $Ga_{(1-x)}In_xSb$ alloys by vertical Bridgman configuration. The results showed that by using magnetic fields of 2mT and 3mT, they succeeded to maintain the radial segregation constant along the 8% ingot and to decrease it for the 3% one. The application of an alternating magnetic field was also experimentally investigated by C. Diaz et al. [8] to see its effect to decrease radial segregation towards the end of the ingot, revealing a good mixture of the molten material.

Li et al [9] investigated experimentally the influence of a high magnetic field on columnar dendrite growth during the directional solidification of Bridgman. They proved that the magnetic field changes the dendrite growth significantly. Also, they proved that for the MnBi dendrite, an axial high magnetic field enhanced the growth of the primary dendrite arm along the solidification direction and at a lower growth speed, a high magnetic field is capable of causing the occurrence of the columnar-to-equiaxed transition (CET). Moreover, it has also been observed that a high magnetic field affects the growth of the high-order dendrite arms of the $\alpha - Al$ dendrite at a higher growth rate. The above results may be attributed to the alignment of the primary dendrite arm under a high magnetic field and the effect of a high magnetic field on crystalline anisotropy during directional solidification.

Zaïdat et al. [10] studied experimentally the influence of forced convection induced by a travelling magnetic field on the macro-segregation and the grain structure for Al-3.5 wt% Ni alloys. They showed that this configuration can control macro-segregations and, moreover, that the dendritic primary spacing maybe modified by varying the applied field.

More recently, a three-dimensional numerical simulation has been performed by T.J. Jaber et al. [11] to study the growth of $Ge_{0.98}Si_{0.02}$ by the Traveling Solvent Method. They applied axial and rotating magnetic fields to suppress the buoyancy convection, in the $Ge_{0.98}Si_{0.02}$ melt zone. They found, by applying an axial magnetic field of various intensities (2, 10, and 22 mT), that as the axial magnetic field increases, the silicon distribution nearby the growth interface becomes more uniform. In the case of a rotating magnetic field, with different applied rotational speeds (2, 7 and 10 rpm), they found out that such kind of magnetic field has a marked effect on the silicon concentration, which changes its shape from a convex one to a nearly flat shape as the magnetic field intensity increases.

However, one can notice that very few studies were interested in the effect of the cavity cross section shapes on the velocity damping and on the induced magnetic field. As far as we are concerned, the only available works are those of Garandet et al. [5] and Moreau et al. [12]. In these studies, the authors present an asymptotic analytical solution for the flow, in the core region, developed in the high Hartmann numbers limit and a numerical solution. The authors are using a commercial code called FLUX-EXPERT and their solutions are presented for different cross section shapes.

The purpose of the present work is to develop a numerical finite element method, in order to study the influence of the application of a vertical magnetic field on the phenomenon of the natural convection during the solidification of a liquid metal in the artificial crystal growth horizontal Bridgman configuration. Numerical results cover many symmetric and non symmetric cross section shapes (circle, square, lozenge and triangle) and are obtained for perfectly electrically and thermally insulating walls.

The rest of the paper is organized in four sections. In the first one, the mathematical modeling of the problem is presented. Essentially, the equations are two partial derivatives equations coupled with an integral flow conservation equation and it is seen that under the assumptions of the problem, these equations can be summarized as two Poisson equations coupled through their right hand side members. In the second section, the weak integral form of the problem is provided. In the third section, some of the most important obtained results are presented. Mainly, these results put into evidence the development of the electromagnetic breaking of the flow and the building of

the Hartmann and parallel layers, as the Hartmann number increases. Discussions of results and main conclusions are drawn in the fourth and last section.

II. THE MATHEMATICAL MODEL

The studied configuration is an infinite horizontal cylinder, whose cross-section *S* is defined by the equations $z_1(y)$ and $z_2(y)$ of its upper and lower half contours, which is supposed to be filled with an electrically conducting liquid and submitted to an externally applied vertical uniform magnetic field $\vec{B}_0$ (see Fig.1).

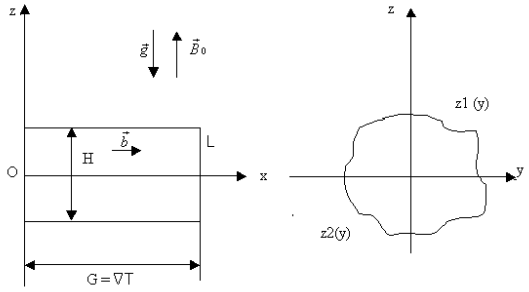

Figure1. Studied configuration in present work

This work is only concerned with the fully established regime of zero flow rate driven by buoyancy. The velocity $\vec{u}$ and the induced magnetic field $\vec{b}$, which is superposed to the applied magnetic field $\vec{B}_0$, are then collinear and directed along the horizontal axis Ox . Under the Boussinesq approximation and in the limit of low Prandtl number, which is completely justified for liquid metals, the velocity and the induced magnetic field satisfy the following linear equations of motion and induction.

$$\vec{\nabla}.\vec{u} = 0 \tag{1}$$

$$\rho_0\, \nu\, \nabla^2\vec{u} = \vec{\nabla}p - \vec{j} \times \vec{B}_0 + \rho_0 \beta G x \vec{g}, \tag{2}$$

$$\nabla^2\vec{b} = -\mu\, \sigma\, (\vec{B}_0 \cdot \vec{\nabla})\vec{u}, \tag{3}$$

Where p, ν, μ, σ, ρ_0, β and $\vec{j}$ denote, respectively, the total pressure, the kinematic viscosity, the magnetic permeability, the electrical conductivity, the density, the thermal dilatation coefficient and the electric current density. It is noticeable that this set of equations does not require any assumption on the value of the magnetic Reynolds number, since $(\vec{b}.\vec{\nabla})$ is identically zero and that $\vec{j} \times \vec{b}$ is a pure gradient incorporated into the definition of the pressure:

$$p = p_{stat} + \rho_0 g z + u\, \frac{b^2}{2} \tag{4}$$

Integrating the projection of equation (2) in the z direction yields

$$p = -\rho_0 \beta G x [z - \bar{z}] g \tag{5}$$

Where the constant $\bar{z}$ has to be such that total flow rate in the cross section S is zero:

$$\iint_S u\, dydz = 0 \tag{6}$$

The equations of the problem can then be summarized as two Poisson equations coupled through their right hand side terms, together with the equation (6), which implicitly determines the constant $\bar{z}$:

$$\Delta u = -\ \frac{\beta G}{\nu}(z - \bar{z}) - \frac{B_0}{\rho_0 \mu \nu}\ \frac{\partial b}{\partial z} \tag{7}$$

$$\Delta b = -\mu \sigma B_0 \frac{\partial u}{\partial z} \tag{8}$$

The boundary conditions are classical. On the contour of the section *S* they imply the no-slip condition ($u = 0$) and the continuity of b. In this work, we limit ourselves to the study of perfectly insulating walls, then, by virtue of Ampere's law $b = 0$.

A. Non Dimensional Form of Equations

It is convenient to use non-dimensional variables based on a typical length H of the section S, on B_0 and on the physical properties of the fluid. For our problem, we prefer to introduce the following variables:

$$Y = y/H \qquad\qquad Z = z/H$$

$$U = \frac{u\, H}{\nu} \qquad\qquad B = \frac{b}{B_0 \mu \sigma \nu}$$

Then, the non dimensional equations of the problem are:

$$\Delta U - Gr(Z - \bar{Z}) + Ha^2 \frac{\partial B}{\partial Z} = 0 \tag{9}$$

$$\Delta B + \frac{\partial U}{\partial Z} = 0 \tag{10}$$

$$\iint_S U\, dYdZ = 0 \tag{11}$$

Where Ha and Gr are the non dimensional Hartmann and Grashoff numbers defined as:

$$Ha = \sqrt{\frac{\sigma}{\rho \nu}} B_0 H \qquad\qquad Gr = \frac{\rho_0 g \beta G H^4}{\nu^2}$$

In general, such an integral-differential set of equations might require long iterative procedure to determine the constant $\bar{Z}$. In the particular case of symmetric sections, the difficulty is easily overcome, because the flow rate is a linear function of $\bar{Z}$. So for symmetric sections $\bar{Z}$ is simply zero. Then, the equations of interest for symmetric cross sections can finally be written as two coupled Poisson equations coupled through their right hand side:

$$\Delta U - Gr\, Z + Ha^2 \frac{\partial B}{\partial Z} = 0 \tag{12}$$

$$\Delta B + \frac{\partial U}{\partial Z} = 0 \tag{13}$$

For non symmetric cross sections, the mathematical model is summarized in three equations.

$$\Delta U - Gr(Z - \bar{Z}) + Ha^2 \frac{\partial B}{\partial Z} = 0 \tag{14}$$

$$\Delta B + \frac{\partial U}{\partial Z} = 0 \tag{15}$$

$$\iint_S U \, dY dZ = 0 \tag{16}$$

Where, $\bar{Z}$ is easily found because, as stated above, the flow is a linear function of $\bar{Z}$, It can be obained by use of the following procedure:

- Choose a first arbitrary value of $\bar{Z}$.
- Calculate the flow, by use of equation (16), with the estimated value of $\bar{Z}$.
- Choose a second arbitrary value of $\bar{Z}$.
- Recalculate the flow with this second value of $\bar{Z}$.
- Calculate $\bar{Z}$ for which the flow equal to zeros.

The last value of $\bar{Z}$ is then used to calculate the velocity and the induced magnetic field.

III. THE VARIATIONAL FORMULATIONS

The strong Galerkin integral formulation of the problem is obtained by multiplying equations (14), (15), and (16), respectively, by two test functions v_1 and v_2 belonging to $H_0^1(\Omega)$ and by integrating over the domain. The weak Galerkin formulation is then obtained after integration by parts of the second order terms and writes:

$$\int_\Omega \left[Ha^2 \frac{\partial B}{\partial Z} v_1 - \left(\frac{\partial U}{\partial Y} \frac{\partial v_1}{\partial Y} + \frac{\partial U}{\partial Z} \frac{\partial v_1}{\partial Z} \right) \right] dY dZ = \int_\Omega Gr\,(Z - \bar{Z})\, v_1 \, dY dZ \tag{17}$$

$$\int_\Omega \left[- \left(\frac{\partial B}{\partial Y} \frac{\partial v_2}{\partial Y} + \frac{\partial B}{\partial Z} \frac{\partial v_2}{\partial Z} \right) + \frac{\partial U}{\partial Z} v_2 \right] dY dZ = 0 \tag{18}$$

The integral form (17)-(18) has been interpolated on linear triangular elements. The unstructured mesh is concentrated near the walls where the Hartmann and the parallel layers are supposed to develop. Since their thickness (Ha^{-1} for Hartmann layers and $Ha^{-1/2}$ for parallel layers) diminishes with increasing Hartmann numbers, the grid densities have been chosen according to the value of the Hartmann number Ha. Grid was refined until solutions were found stable and invariable with further refinements.

IV. NUMERICAL RESULTS

The first numerical test was to validate the developed finite element code. The numerical velocity solution was obtained for the case of circular cross section with $Ha = 10^{-12}$ and $Gr = 10^6$ (see Fig.2). This numerical solution was then compared with the analytical solution presented by Bejan et al. [13] for fully developed natural convective flows in long pipes subject to temperature gradients for the same Grashoff number. The two solutions are in perfect agreement and the validation is thus satisfactory.

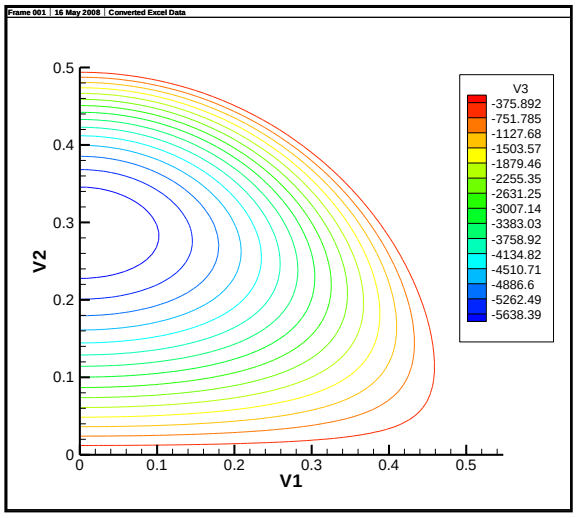

Figure2. Velocity Contours ($Ha = 10^{-12}, Gr = 10^6$)

Then the interest was focused on the variation of the cross section shape. Four shapes were investigated: square, circle, lozenge, and triangle (see Fig. 3) and for the rest of the presented results the Grashoff number is chosen to be $Gr = 10^5$.

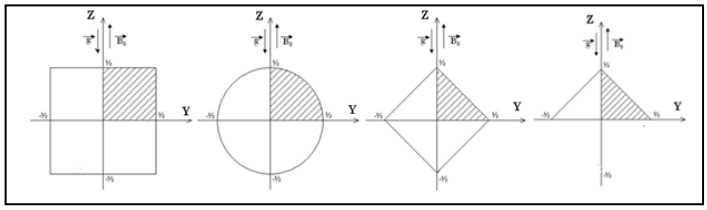

Figure3. Studied cross section shapes

A. *Symmetric cross sections*

Since equations (12)-(13) are linear and that the studied sections are symmetric with regards to axes Y and Z, then the solutions U and B are symmetric with respect to Z and anti-symmetric with respect to Y . Hence, the solution can be obtained only for a quarter of the domain (see Fig. 3). Figures (4), (5) and (6) show the contours of the non dimensional velocity field in circular, square and lozenge cross sections, respectively.

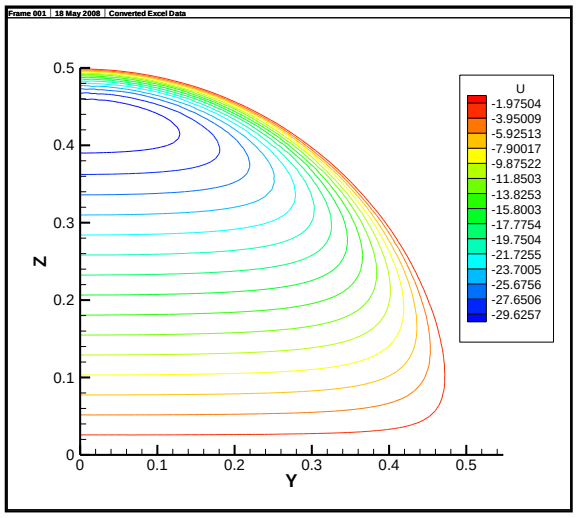

(a)

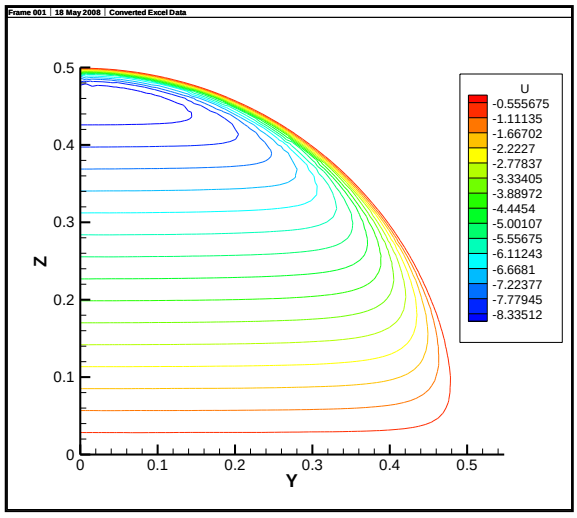

(b)

Figure4. Contours of the velocity for a) Ha = 5 and b) Ha = 100 (circular cross section)

The electromagnetic braking of the Lorentz forces is obvious on the figures. As the Hartmann number increases, which is a direct result of the magnetic field magnitude increase, one can see the drastic decrease of the velocity magnitude for the three shapes. Moreover, the development of the Hartmann layers for the three cross sections is seen on the figures. These layers which develop in the normal direction to the magnetic field have a thickness of the order of Ha^{-1}.

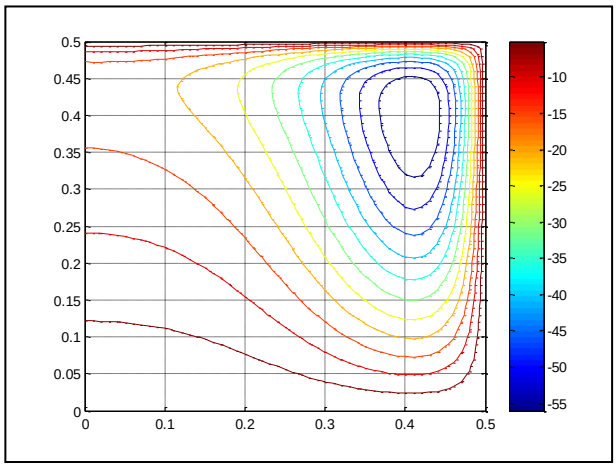

(a)

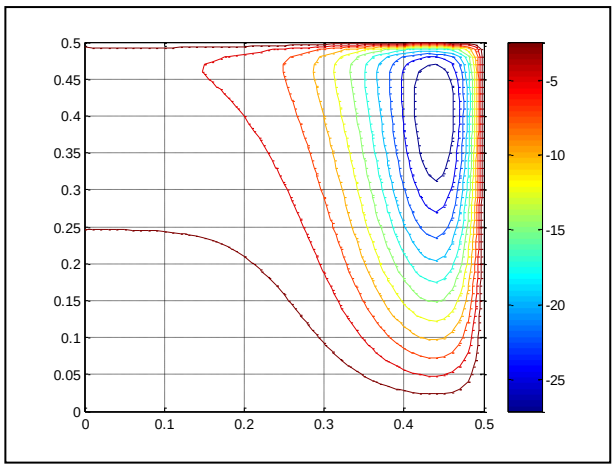

(b)

Figure5. Contours of the velocity a) Ha = 50 and b) Ha = 100 (square cross section)

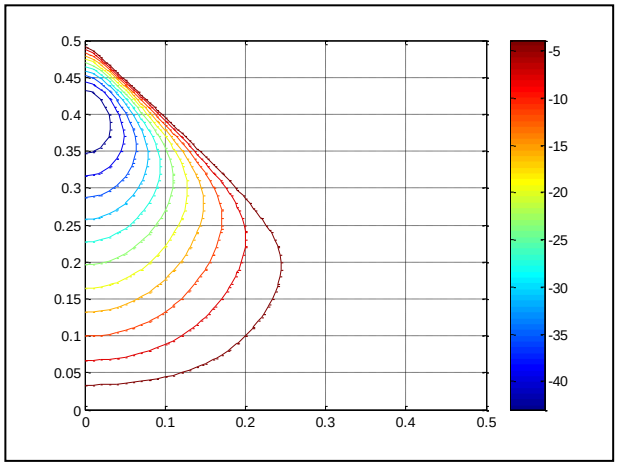

(a)

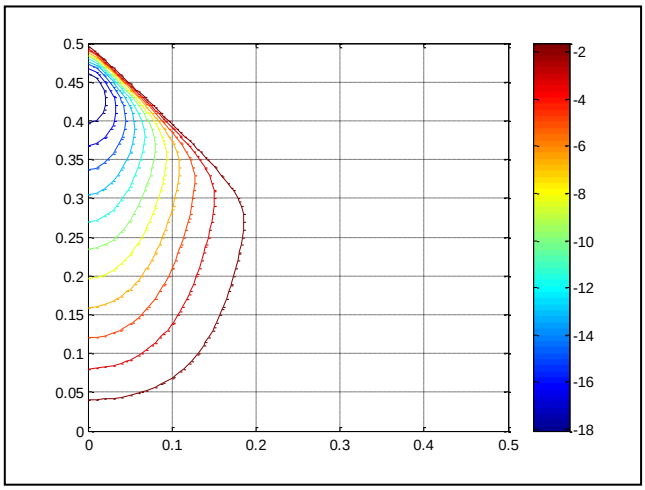

(b)

Figure6. Contours of the velocity for a) Ha = 50 and b) Ha = 100 (lozenge cross section)

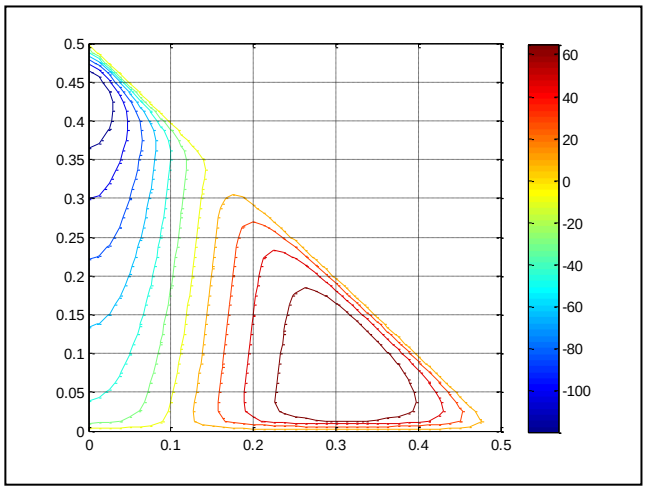

(b)

Figure7. Contours of the velocity for a) Ha = 50 and b) Ha = 100 (triangular cross section)

For the square section, an over velocity is present, near the boundaries that are parallel to the magnetic field direction. These over velocities are the signature of the presence of two parallel layers having a thickness of $Ha^{-1/2}$. Results have been compared to the asymptotic solution shown in Garandet et al. [5] and to the numerical solution obtained by Moreau et al. [12] by a commercial code. The predictions obtained with the genuine method suggested here show a quite good agreement.

B. Non symmetric cross section

Since equations (14)-(15) are symmetric and that the studied sections are symmetric with regards to axe Z, then the solutions U and B are symmetric with respect to Z and the solution can be obtained only for half of the domain (see Fig. 3). Figure (7) shows the contours of the non dimensional velocity field for the triangular section.

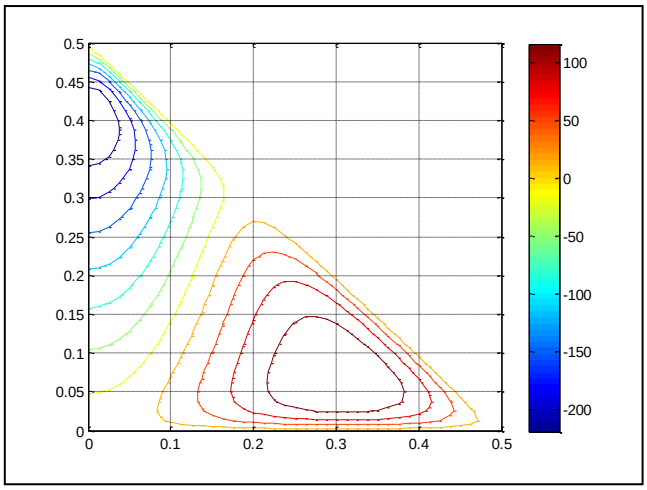

(a)

For the triangular cross section, it is noticeable that the flow is made following two directions: x-negative direction in a part of the studied section and in the x-positive direction in the rest of the section.

For small Ha numbers, this flow horizontally divides the cross section in two zones and the higher Ha is, the more the limitation between the two zones is directed towards the vertical line.

Also we can observe the building up of the Hartmann layer along the horizontal wall and along the top of the oblique wall.

V. CONCLUSION

In this work, a numerical finite element method for the solution of the magneto hydrodynamic problem associated with the study of the electromagnetic damping of the natural convection in the crystal growth horizontal Bridgman configuration is presented. The resulting code is validated through the comparison of its numerical results with analytical ones obtained without any magnetic field. Numerical results have been obtained for four cross section shapes: circular, square lozenge and triangular. For a given Grashoff number Gr, the Hartmann number Ha has been systematically modified to underline the electromagnetic damping and the associated building of the Hartmann and the parallel layers.

REFERENCES

[1] K. Hoshikawa, H. Hirata, H. Nakanishi, and K. Ikuta, "Control of oxygen concentration in CZ silicon growth" , Proceedings of the 4th International Symposium on Silicon Matter Science Technology, NJ, pp. 101-112. Vol. Semiconductor Silicon ,1981.

[2] K.M. Kim, G.H. Schwuttke and P. Smetana, "Apparatus for Czochralski silicon crystal growth through axial magnetic field fluid damping", IBM Tech. Duscl. Bu 24 3376-3377,1981.

[3] T.A. Campbell and J.N. Koster, "Radioscopic visualization of indium antimonide growth by the vertical Bridgman-Stockbarger technique", Journal o Crystal Growth 147 pp. 408-410 , 1995.

[4] L. Davoust, R. Moreau, M.D. Cowley, P.A. Tanguy, and F. Bertrand, "Numerical and analytical modelling of MHD driven flow in a Bridgman crystal growth configuration", Journal of Crystal Growth, pp. 422-432, 1995.

[5] J. P Garandet, T. Alboussiére , and R. Moreau, "Buoyancy driven convection in a rectangular enclosure with a transverse magnetic field", J. of Heat and Mass Transfer ,Vol. 35 N° 4, pp. 741-748, 1992.

[6] B. H. Dennis , G. S. Dulikravich, "Magnetic field suppression of melt flow in crystal growth", International Journal of Heat and Fluid Flow, 23 269–27, 2002.

[7] A. Mitric, T. Duffar, C. Diaz-Guerra, V. Corregidorc, L.C. Alves, C. Garnier and G. Vian, "Growth of $Ga_{(1\_x)}In_xSb$ alloys by Vertical Bridgman technique under alternating magnetic field", Journal of Crystal Growth ,287 224–229, 2006.

[8] C. Díaz-Guerra, A. Mitric, J. Piqueras and T. Duffar, "Cathodoluminescence mapping and spectroscopy of Te-doped InxGa1-x Sb grown by the vertical Bridgman method under an alternating magnetic field", article in press in Superlattices and Microstructures, 2008.

[9] X. Li, Y. Fautrelle and Z. Ren, "Influence of a high magnetic field on columnar dendrite growth during directional solidification", Acta Materialia , 55 5333–5347, 2007.

[10] K. Zaïdat, N. Mangelinck-Noël and R. Moreau, "Control of melt convection by a travelling magnetic field during the directional solidification of Al–Ni alloys", C. R. Mecanique, 55 pp 335, 2007.

[11] T.J. Jaber, M.Z. Saghir and A. Viviani, "Three-dimensional modelling of GeSi growth in presence of axial and rotating magnetic fields", European Journal of Mechanics B/Fluids, article in press, 2008.

[12] Moreau, T. Alboussière, N. Ben Salah, J.P. Garandet, R. Bolcato and A.M. Bianchi, "MHD Control of Free Convection in Horizontal Bridgman Crystal Growth", Magnetohydrodynamics (Magnitnaya Gidrodinamika), Vol. 30, N° 3, pp. 282-288, 1994.

[13] A. Bejan and C.L.Tien, "Fully developed natural counter flow in a long horizontal pipe with different end temperatures", Int. J. Heat Mass Transfer, 21, 6 pp. 701-708 , 1977.